

Carbon dioxide exchange over multiple temporal scales in an arid shrub ecosystem near La Paz, Baja California Sur, Mexico

TOM W. BELL*[†], OLAF MENZER[‡], ENRIQUE TROYO-DIÉQUEZ[§]
and WALTER C. OECHEL*

*Global Change Research Group, Department of Biology, San Diego State University, San Diego, CA 92182, USA, [†]Earth Research Institute, University of California Santa Barbara, Santa Barbara, CA 93106, USA, [‡]Department of Geography, University of California Santa Barbara, Santa Barbara, CA 93106, USA, [§]Centro de Investigaciones Biológicas del Noroeste, S.C. La Paz, Baja California Sur 23090, Mexico

Abstract

Arid environments represent 30% of the global terrestrial surface, but are largely under-represented in studies of ecosystem carbon flux. Less than 2% of all FLUXNET eddy covariance sites exist in a hot desert climate. Long-term datasets of these regions are vital for capturing the seasonal and interannual variability that occur due to episodic precipitation events and climate change, which drive fluctuations in soil moisture and temperature patterns. The objectives of this study were to determine the meteorological variables that drive carbon flux on diel, seasonal, and annual scales and to determine how precipitation events control annual net ecosystem exchange (NEE). Patterns of NEE from 2002 to 2008 were investigated, providing a record with multiple replicates of seasons and conditions. Precipitation was extremely variable (55–339 mm) during the study period, and reduced precipitation in later years (2004–2008) appears to have resulted in annual moderate to large carbon sources (62–258 g C m⁻² yr⁻¹) in contrast to the previously reported sink (2002–2003). Variations in photosynthetically active radiation were found to principally drive variations in carbon uptake during the wet growing season while increased soil temperatures at a 5 cm depth stimulated carbon loss during the dry dormant season. Monthly NEE was primarily driven by soil moisture at a 5 cm depth, and years with a higher magnitude of precipitation events showed a longer growing season with annual net carbon uptake, whereas years with lower magnitude had drier soils and displayed short growing seasons with annual net carbon loss. Increased precipitation frequency was associated with increased annual NEE, which may be a function of increased microbial respiration to more small precipitation events. Annual precipitation frequency and magnitude were found to have effects on the interannual variability of NEE for up to 2 years.

Keywords: arid ecosystem, carbon exchange, ecosystem memory, eddy covariance, interannual variability, precipitation

Received 27 September 2011 and accepted 21 February 2012

Introduction

Arid and semi-arid regions comprise 30% of the global terrestrial surface (Asner *et al.*, 2003; Lal, 2004) and are expanding due to global climate change and anthropogenic disturbance (Schlesinger *et al.*, 1990; Eswaran *et al.*, 2000; Huenneke *et al.*, 2002; Emmerich, 2003), but despite their unique environmental characteristics and importance (Unland, 1996; Lal, 2004), arid environments are understudied in relation to carbon flux measurements and global terrestrial carbon calculations. There are currently over 500 participating eddy covariance sites studying CO₂ fluxes from about 30

regional networks operating on a long-term basis in the FLUXNET network (Baldocchi *et al.*, 2001); however, globally, only nine of these sites are located in hot arid/desert environments. Although there have been studies using the eddy covariance technique in arid climates (Hastings *et al.*, 2005; Arneth *et al.*, 2006; Wohlfahrt *et al.*, 2008; Rotenberg & Yakir, 2010), there has been no publication of long-term data sets from any FLUXNET sites, despite the clearly stated need and importance (Goulden *et al.*, 1996; Baldocchi & Wilson, 2001; Barford *et al.*, 2001; Ma *et al.*, 2007).

Long-term analysis of data sets can help to explain interannual variability and seasonality of carbon exchange in water limited ecosystems (Luo *et al.*, 2007; Ma *et al.*, 2007; Archibald *et al.*, 2009). Precipitation pulses can rapidly increase soil moisture and can

Correspondence: Tom W. Bell, tel. + 619 857 1233,
fax + 619 594 7831, e-mail: thomas.bell@lifesci.ucsb.edu

stimulate the low carbon exchange rates of arid systems resulting in dramatic variation in fluxes between seasons and years (Huxman *et al.*, 2004; Hastings *et al.*, 2005; Allard *et al.*, 2008). Not surprisingly, significant increases in production have been tied to greater precipitation (Seely & Louw, 1980); however, the influence of past (i.e. >1 year) precipitation pulses on annual patterns of net ecosystem exchange (NEE, Odum, 1969) is still poorly explored, and multi-year studies exploring the impact of 'ecosystem memory' on carbon exchange are few despite the fact that carbon exchange can be affected by the conditions of antecedent years (Schwinning *et al.*, 2004). There are multiple dynamics possible. In one, high decomposition rates, due to above average precipitation, can increase the subsequent availability of inorganic nutrients (Barford *et al.*, 2001). In another, gradual changes in dominant vegetation or community structure change the ecosystem's ability to sequester carbon (Connin *et al.*, 1997; Huenneke *et al.*, 2002). Surprisingly, due to the relatively low number of eddy covariance measurement sites, and long-term analyses from arid regions, even the magnitude of arid-zone ecosystem carbon exchange is poorly understood, and there has been a strong suspicion that large reported carbon uptake values previously reported for desert ecosystems may be unverified by carbon stock quantification and potentially balanced with large losses in subsequent years (Schlesinger *et al.*, 2009).

Climate change can alter the dynamics of carbon sequestration in arid environments that already exist under extreme water and temperature stress. Change in water use efficiency [from, e.g. increases in atmospheric CO₂ (Grunzweig *et al.*, 2003)], precipitation, and temperature all have potentially large impacts on NEE of arid ecosystems. Shifting precipitation can change NEE patterns as plants and soil microbes differ in their response to soil moisture variability (Potts *et al.*, 2006), where shifts in moisture timing and frequency can have increased effects on respiration. Increased temperatures show a negative correlation with green vegetation in arid ecosystems and depress carbon sequestration through direct and indirect negative effects on plant growth, such as increased maintenance energy use and water stress, respectively (Ryan, 1991; Braswell *et al.*, 1997), while increased temperature also stimulates soil respiration (Xu & Qi, 2001).

The objective of this study is to quantify the magnitude and interpret the patterns of net ecosystem exchange over varying temporal scales in an arid-zone shrub community using eddy covariance (Hastings *et al.*, 2005). The site is located in an arid shrub reserve, 15 km west of La Paz, Baja California Sur, Mexico. A previous study measured NEE over a 24 month period

between 2002 and 2003 with a net ecosystem uptake of 39 g and 52 g C m⁻² yr⁻¹ in 2002 and 2003, respectively. In this study, the effects of diel, seasonal, and interannual patterns of NEE were investigated from January 2004 to December 2008, with the addition of data from the earlier study to elucidate seasonal and interannual trends. This 7 year data set is the longest such record and analysis of any hot desert FLUXNET site (Vargas & Yezpez, 2011). This record is sufficiently long to provide multiple replicates of seasons and conditions, thereby allowing the identification of significant meteorological drivers that control not only seasonal changes in carbon flux but also the interannual variation in seasonal fluxes that occur, and multiple annual NEE estimates can be compared to variable precipitation events over several years.

To investigate the environmental controls on seasonal variation in fluxes as well as the interannual variation in seasonal fluxes, objectives included: (1) Determine the major meteorological variables and how they correlate with diel carbon flux patterns during the growing and dormant seasons; (2) Determine how the magnitude and frequency of precipitation events affect the annual cumulative NEE of this ecosystem; (3) Determine if the precipitation of antecedent years is strongly correlated with annual NEE and, if so, how long this effect lasts.

Materials and methods

Site description

The study site is located in the La Paz-El Carrizal basin about 15 km west of the city of La Paz, Baja California Sur, Mexico (24°07' N, 110°26' W), and is part of the desert terrestrial experimental reserve of the Centro de Investigaciones Biológicas del Noroeste (CIBNOR). The climate is very dry and hot and is characterized as a hot desert climate by Köppen's Climate Classification System (García, 1973). Annual precipitation is variable with a majority of rainfall delivered by monsoons in August through September with occasional minor precipitation events occurring from October to February. The highest mean temperatures occur between July and September with the highest radiation from April to August (Troyo-Diéquez *et al.*, 1990). Mean annual precipitation and temperature over an 84 year period were 181.8 mm and 23.6°C; the maximum recorded average annual temperature was 25.7°C, in 1963, and the maximum precipitation was 622 mm, in 1943, with a historical median calculated at 156.6 mm (CONAGUA, 2011). The impact of global warming across northwestern Mexico is difficult to analyze because long-term climatic data series are lacking, and this region is subject to strong seasonal variability (Gutiérrez-Ruacho *et al.*, 2010).

The site lies on alluvial plains formed by granite deposits carried from the nearby Sierra de la Laguna Mountains.

Numerous dry streambeds, known as arroyos, traverse the flat plain and are subject to flooding only after heavy rain. The soils are sandy, deep, and well drained and are classified as Yermosols, Xerosols, and Regosols (Maya & Arriaga, 1996). Bulk density is 1.6 g cm^{-3} , with a sand, clay, and silica content of 76%, 16%, and 13%, respectively. Over a 1.5 m depth profile, soil organic matter was 0.21% and soil nitrogen 0.02% (Hastings *et al.*, 2005).

The vegetation is classified as a sarcocaulous scrub and lies at the extreme southern end of the Central Gulf Coast Sub-division of the Sonoran Desert (Shreve & Wiggins, 1964; Brown & Lowe, 1980; León de la Luz *et al.*, 2000). Perea *et al.* (2005) found four morphological groups in the study area: (1) crassicaulescent plants, or succulent cacti, (2) sarcocaulous species, (3) woody trees, and (4) woody shrubs. Cacti and sarcocaulous plants dominate in the open scrub, woody shrubs dominate in the clustered scrub, and woody trees, together with all the previous life forms, form the more mesic closed scrub. The dominant community in La Paz coastal area is composed by nine plant species including three trees (*Prosopis articulata*, *Cyrtocarpa edulis*, *Bursera microphylla*), four shrubs (*Jatropha cinerea*, *J. cuneata*, *Fouquieria diguetii*, *Larrea tridentata*), and columnar cacti (*Pachycereus pringlei*, *Stenocereus thurberi*). With the exception of the phreatophyte *P. articulata* and *L. tridentata*, which are evergreen, the major tree and shrub species are leafless for at least 5 months of the year. The average canopy height was measured at 2–3 m, with *P. pringlei* representing the tallest species at 6–8 m.

Eddy covariance

Net ecosystem carbon dioxide and water vapor exchange were measured using the eddy covariance method from January 2002 to December 2008 (Baldocchi *et al.*, 1988; Baldocchi, 2003). The eddy covariance system was composed of a fast response (10 Hz) three-dimensional sonic anemometer–thermometer (Wind Master Pro, Gill Instruments, Lymington, UK) and a fast response (10 Hz) open path gas analyzer (LI-7500; LI-COR, Lincoln, NE, USA), both instruments mounted on a tower at 13 m above the ground. Data were transmitted by fiber optic cable to the main campus of CIB-NOR, and half-hourly mean $\text{CO}_2/\text{H}_2\text{O}$ fluxes were calculated as the covariance between the vertical wind speed and the $\text{CO}_2/\text{H}_2\text{O}$ mixing ratio using the postprocessing software EDIRE (University of Edinburgh). Air density fluctuations were corrected following Webb *et al.* (1980). A correction for the self-heating of the open path infrared gas analyzer was not included as this was found to result in an underestimation of NEE in arid systems (Wohlfahrt *et al.*, 2008).

The rejection criteria used to screen data postprocessing included rain events, incomplete 30 min data collection, and spikes of CO_2 , H_2O , and/or temperature variance greater than 2 SD from the mean. A critical friction velocity (u^*) threshold was set at 0.15 m s^{-1} , for both day and night, and was determined as the point where increases in u^* had little effect in apparent CO_2 flux. On an annual basis, the average coverage in flux data was 62.6%, very close to the average yearly rate of 65% for FLUXNET studies (Falge *et al.*, 2001).

Energy balance closure was used as one parameter to assess the performance of the eddy covariance system (McMillen 1998; Luo *et al.*, 2007). For each year, the summed half-hour values of sensible heat flux (H) and latent heat flux (LE) were regressed against net radiation (R_n) minus soil heat flux (G). The goodness of fit was quantified with an average R^2 of $.846 \pm .015$ and an average energy closure of 81% over the 5 years studied. These values are similar to what has been reported for most FLUXNET sites (Wilson *et al.*, 2002).

Data processing: gap-filling, random uncertainties, and flux-partitioning

Gap-filling was performed using the Marginal Distribution Sampling (MDS) approach (Reichstein *et al.*, 2005). In the MDS method, gaps are filled using a moving look-up table with flexible window sizes on adjacent data points measured under similar meteorological conditions. Small gaps are filled using linear interpolation. A large 184 days gap in the latter half of 2003 and 2006 was not filled, as it was too large to estimate with confidence.

Random uncertainties could also be inferred from the MDS algorithm as the SD of values in the moving window estimate used for gap-filling. For actually measured data, the uncertainties were calculated by constructing an 'artificial gap' and then using the standard procedure. Annual aggregates of random uncertainties were calculated as the SD of 10 000 Monte Carlo random samples based on a Smith Sigmoid light response (during daytime growing season) and a Lloyd–Taylor respiration model (during dormant season). Parameters of the model were constrained on the months with the lowest SE, and the random samples were taken from a double exponential distribution.

Monthly means of half-hour flux data over the diurnal cycle were then used to calculate monthly and annual sums (Grunzweig *et al.*, 2003). Partitioning of NEE into the two component fluxes GPP and R_{eco} was performed by calculating the nighttime-based estimate of R_{eco} , fitting Lloyd–Taylor models for temperature sensitivities and extrapolating to daytime periods (Reichstein *et al.*, 2005). Gap-filling, flux-partitioning, and the uncertainty estimates were all processed by the online tool available at <http://www.bgc-jena.mpg.de/~MDIwork/eddyproc/>. U^* biases were determined as the difference in the annual sum when gap-filled including the values removed through u^* -filtering (Morgenstern *et al.*, 2004).

Meteorological data

The following micrometeorological variables were averaged over half-hour intervals from observations made every 10 s and stored using a datalogger (CR-23X; Campbell Scientific Inc, Logan, UT, USA): air temperature and relative humidity (RH) (HMP-45; Vaisala Inc., Helsinki, Finland) at 2, 6, and 9 m above the ground; wind vector (Wind Monitor; R.M. Young Company, Traverse City, MI, USA) at 2, 6, and 9 m above the ground; photosynthetically active radiation (PAR) (LI-190SB; LI-COR, Lincoln, NE, USA) at 5 m above the ground; net radiation (R_n) (Q-7.1; REBS Inc., Seattle, WA, USA) at 2 m above

the ground on a mast separated by 15 m from the tower; soil heat flux (HFT-3.1; REBS Inc.) at a depth of 5 cm; soil temperature (Type T; Omega Engineering Inc., Stamford, CT, USA) and volumetric soil moisture (CS-615; Campbell Scientific Inc., Logan, UT, USA) were measured at depths of 5, 10, 20, 30, 40, 50, 75, and 150 cm at a distance of 15 m from the tower; and precipitation (TE525MM; Texas Electronics Inc., Dallas, TX, USA) at a distance of 6 m from the tower.

Remote sensing analysis

Normalized difference vegetation index (NDVI) of the arid shrub reserve was calculated using the software ENVI (Version 4.8; Exelis, Boulder, CO, USA) from Landsat 4-5 TM images from July and November for the years 2001, 2002, and 2005–2008. July and November dates were chosen because they represent dates with a canopy minimum and maximum, respectively. The difference in NDVI value between July and November for each year was used as a proxy for canopy development.

Statistical analysis

Statistical analysis was performed with the statistical software SYSTAT (Version 12; Cranes Software Inc., Chicago, IL, USA) and MATLAB (7.12; MathWorks, Natick, MA, USA). For diel flux pattern analysis, forward, stepwise multiple linear regressions were performed to determine significant meteorological variables to half-hour averaged carbon flux for each measured month. Once the significant variables were determined, the correlation coefficient of each variable to carbon flux was found by simple linear regression. The variables with the largest R^2 values were selected as the most important meteorological variables to carbon flux for each month. Months that possessed a similar hierarchy of significant variables to carbon flux were categorized into seasons.

Seasonal carbon flux analysis consisted of forward, stepwise multiple linear regressions to determine significant monthly meteorological variables to monthly summed NEE. Significant variables were identified, and the correlation coefficient of each variable to monthly NEE was found by simple linear regression. Months were then grouped by season, as determined by the diel analysis, to determine if a seasonal response to the significant variable was present.

To determine how precipitation influences interannual variability in NEE, the correlation with rain events from the current and four antecedent years was tested. After identifying the timeframe that was most supported by the data, the next step was taken in modeling annual NEE as a response to frequency and magnitude of precipitation events. The relationship was modeled over multiple timespans to investigate the temporal scale of the ecosystem memory at the measurement site. The magnitude of a precipitation event was calculated on a daily basis as the accumulated sum over adjacent days with precipitation >0 mm. Several thresholds for the definition of an actual rainfall event were considered, ranging from 1 to 4 mm. The data were normalized to rank the relative importance of drivers of interannual variation in NEE.

Results

Meteorological conditions

Average annual temperature across the study period was fairly constant at $23.1 \pm 0.2^\circ\text{C}$, close the historical average of 23.6°C . R_{net} was also similar across years with an annual average of $117.0 \pm 6.4 \text{ W m}^{-2}$ and showed a similar pattern of a summer maximum and winter minimum as previously reported at this site (Hastings *et al.*, 2005) (Fig. 1). PAR and RH also remained stable across years with annual averages of $473.9 \pm 28.7 \mu\text{mol m}^{-2} \text{ s}^{-1}$ and $58.9 \pm 1.7\%$, respectively.

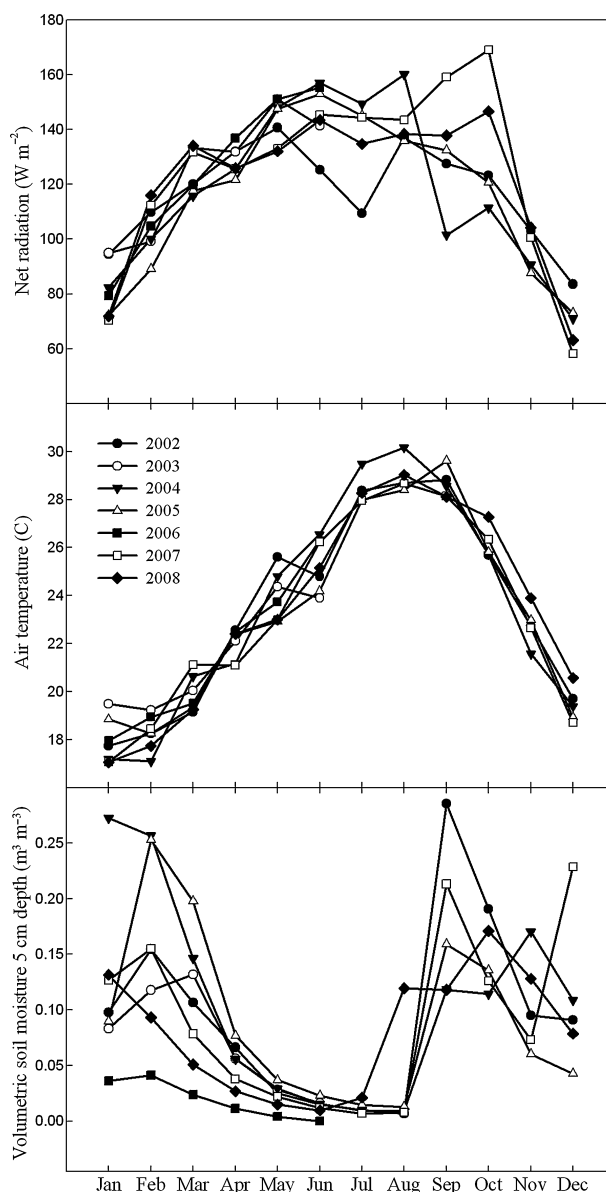


Fig. 1 Monthly averages of net radiation, air temperature at 2 m, and soil moisture at a depth of 5 cm over each study year.

Precipitation varied greatly among the study years with a maximum of 339 mm recorded in 2001 and a minimum of 55 mm in 2005. Late summer monsoon events accounted for 82% of annual precipitation on average with events ranging from a total of 320 mm in 2001 to 41 mm in 2005 (Table 1).

Remote sensing analysis

The difference in NDVI from July to November, used as a proxy for canopy development, was linearly regressed against the amount of precipitation between the image dates. This yielded a significant result in which greater precipitation led to increased canopy development ($R^2 = 0.69$, $P = 0.04$).

Controls of diel and seasonal flux patterns

Apparent controls over diel carbon flux were elucidated with the examination of average monthly carbon flux patterns (Fig. 2) against the patterns of meteorological drivers. Multiple significant meteorological variables to carbon flux were identified for each measured month; however, either PAR or soil temperature at a depth of 5 cm (ST5) was found to have the strongest correlation in 64 of the 72 measured months. The principle driver of carbon flux on a diel time scale was used to differentiate the seasonality of any particular month. Months in which half-hour average PAR was the strongest correlate controlling a sustained daylight CO_2 uptake were categorized as the growing season (typically September to April), whereas months in which half-hour average ST5 was the strongest correlate to an increasing daylight CO_2 efflux were categorized as the dormant season (typically May to August) (Fig. 3). Months classified as belonging to the growing season were always net carbon sinks with an average NEE

of $-10.85 \pm 10.2 \text{ g C m}^{-2}$ ($n = 22$), whereas months classified as part of the dormant season were for the large part net carbon sources with an average NEE of $16.27 \pm 8.6 \text{ g C m}^{-2}$ ($n = 42$).

During January 2004, a month that was classified as the growing season, average diel carbon uptake was closely correlated with available PAR throughout the daylight period ($R^2 = 0.62$, $P < 0.001$) with a monthly NEE of -39 g C m^{-2} (Fig. 3a). In July 2005, during the dormant season, average diel carbon flux followed the increase in ST5 ($R^2 = 0.56$, $P < 0.001$), with a monthly NEE of 20.5 g C m^{-2} (Fig. 3b). A similar pattern was found during all months throughout the study period, except those that included a moderate precipitation event ($>5 \text{ mm}$) and followed the dormant season. In these months, soil moisture at a depth of 5 cm was the strongest significant correlate to carbon efflux with ST5 also displaying a high R^2 value. These months were classified as storm months and displayed relatively large carbon sources and had an average NEE of $23.71 \pm 8.8 \text{ g C m}^{-2}$ ($n = 8$).

Using the strongest significant meteorological correlate to diel carbon flux allowed for a comparison of monthly NEE magnitude vs. season (Fig. 4). Growing season months, with their high PAR correlation and negative NEE, gradually gave way to dormant season months, which displayed high correlation with ST5 and positive NEE values. The dormant season was then interrupted by one or multiple storm months, which showed increased monthly NEE values, then transitioned back to growing season months. This pattern was seen throughout the study period but the length of each season varied between years. For example, the year 2002 began with four growing season months with gradually decreasing monthly carbon sinks until moving into a 4 month summer dormant season with increasing carbon sources. A large precipitation event

Table 1 Inter-annual variability of annual net ecosystem exchange (NEE) estimated from eddy covariance along with annual and late summer (July–October) precipitation. Note the effect of precipitation on NEE of the current and subsequent year. Annual random uncertainties for the years 2002, 2004, 2005, 2007 and 2008 are indicated by 1 standard deviation of the Monte Carlo resampling approach based on half-hourly uncertainties. For 2006 the annual NEE and the uncertainty (1 SD) are estimated by the interannual variability model driven by the frequency and magnitude of precipitation events. U* biases represent the difference in the annual sum when gap-filled, including the values removed through u*-filtering (Morgenstern *et al.*, 2004).

Year	NEE ($\text{g C m}^{-2} \text{ yr}^{-1}$)	U* Bias ($\text{g C m}^{-2} \text{ yr}^{-1}$)	Annual precipitation (mm)	Late summer precipitation (mm)
2001	ND	ND	339	320
2002	-39 ± 2.2	-16.9	147	93
2003	-52	ND	196	189
2004	62 ± 2.5	-68.4	123	80
2005	258 ± 1.8	-37.2	55	41
2006	171 ± 52.9	ND	179	128
2007	96 ± 1.6	-23.7	177	154
2008	150 ± 1.7	-16.6	105	78

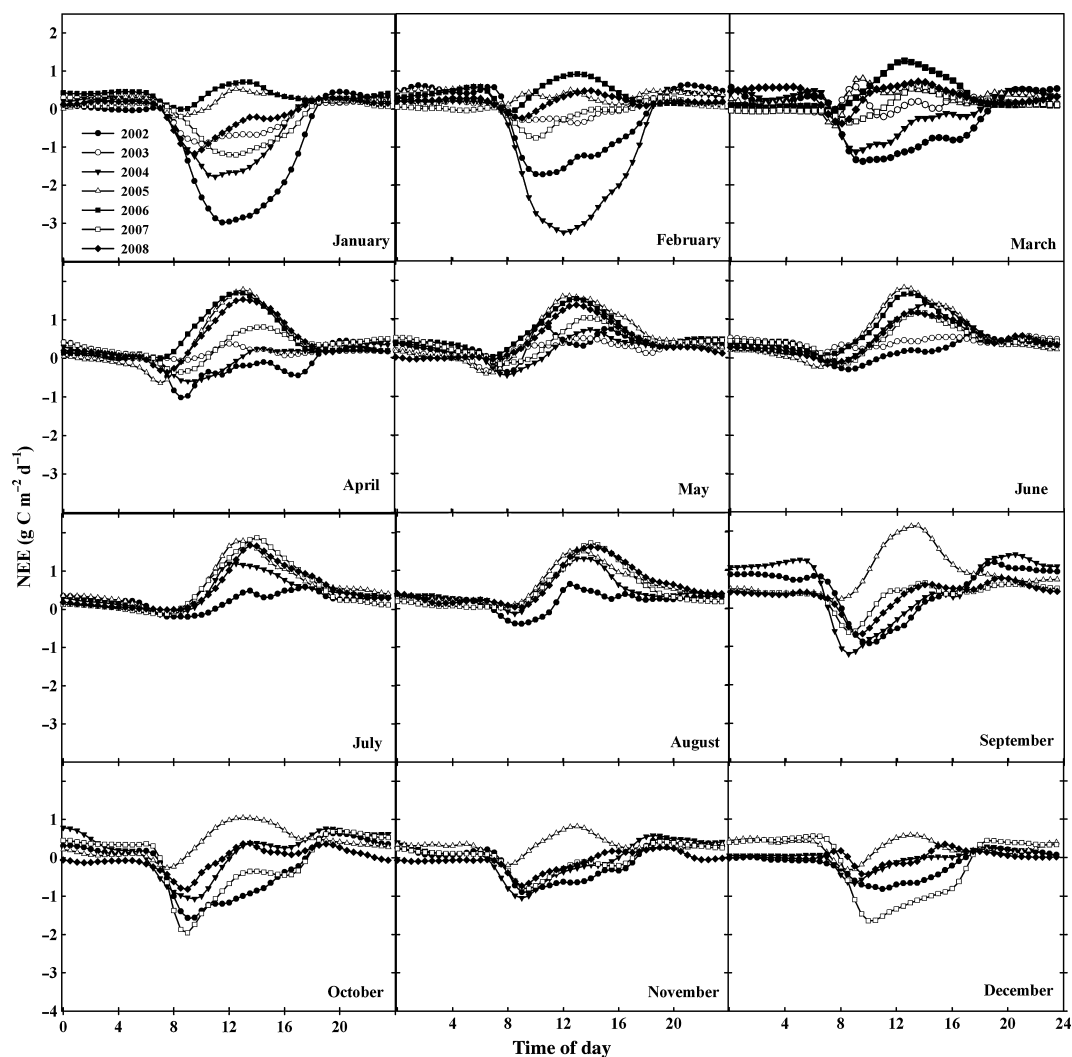


Fig. 2 Average diel carbon pattern for each month in the study period.

occurred in September leading to a storm month, then a transition back to the growing season (Fig. 4a). In contrast, the year 2005 displayed 10 dormant season months interrupted by two storm months with no transition to a growing season throughout the year (Fig. 4b). All months in year 2005 were carbon sources.

Drivers of seasonal variation were determined by the examination of monthly summed NEE against monthly average environmental conditions. The strongest significant correlate to growing and dormant season months was volumetric soil moisture at a depth of 5 cm. A regression of average monthly soil moisture at a depth of 5 cm correlated well with monthly NEE across all years, where greater soil moisture led to greater ecosystem carbon uptake, while months with drier soils showed larger carbon sources ($R^2 = 0.53$, $P < 0.01$) (Fig. 5). The annual course of carbon flux through the study years clearly illustrates the seasonality of the

ecosystem and the variation between years (Fig. 6). Flux-partitioning analysis indicates high GPP during the growing season months at the start of the year and carbon loss during the summertime dormant season months. A spike in ecosystem carbon loss and ecosystem respiration is also visible during the storm month, which then transitions to net carbon uptake and increased GPP during the growing season.

Controls of interannual variability of NEE

The variability of both annual precipitation and NEE was high during the years 2002–2008, with annual net carbon exchange ranging from $-52 \text{ g C m}^{-2} \text{ yr}^{-1}$ in 2003 to $258 \text{ g C m}^{-2} \text{ yr}^{-1}$ in 2005, with a mean of $79 \pm 117 \text{ g C m}^{-2} \text{ yr}^{-1}$ (Table 1). Random uncertainties associated with the measurements ranged from 3.1 to $5.0 \text{ g C m}^{-2} \text{ yr}^{-1}$ (95% confidence level). These

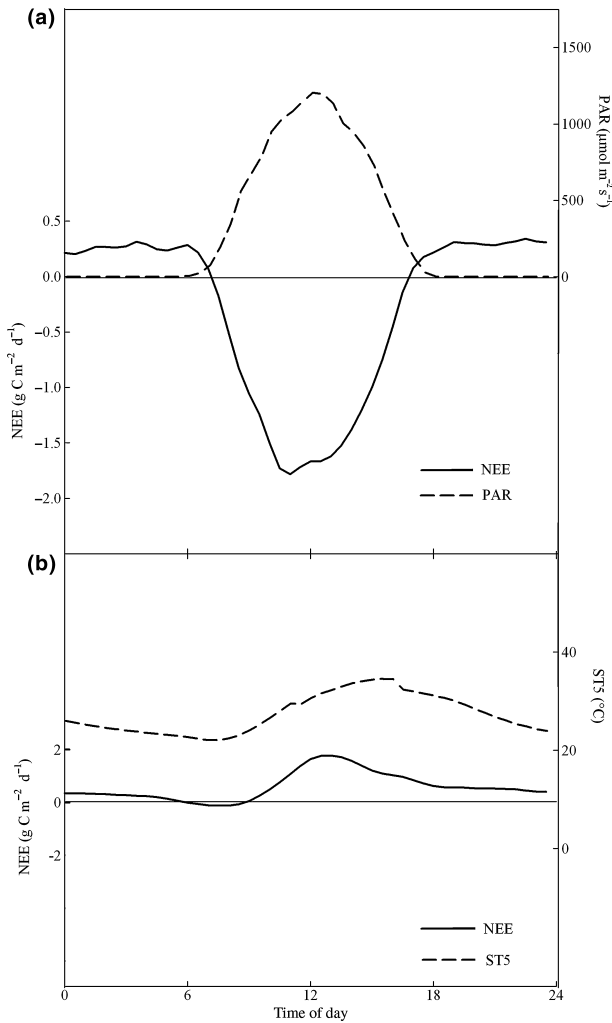


Fig. 3 (a) January 2002, a growing season month, average diel carbon flux (NEE) shown by the solid line and photosynthetically active radiation shown by the dashed line. (b) In July 2005, a dormant season month, average diel carbon flux (NEE) shown by the solid line and soil temperature at a depth of 5 cm (ST5) shown by the dashed line.

uncertainties scaled with carbon flux magnitudes on the half-hourly timescale, which is typical for eddy covariance data and in agreement with previous studies (Richardson *et al.*, 2008). Uncertainty was not determined for year 2003 as 6 months of flux data were missing, the annual sum was taken from Hastings *et al.*, 2005. U^* biases were negative for every measured year, and this was expected as u^* filtering seeks to correct for nonmeasured respiration due to low turbulent mixing.

Annual NEE sums showed a strong correlation with precipitation sums of the previous years. Up to 81% of the variability could be explained by only taking into account the current year and the antecedent year precipitation as independent variables. Increased precipitation in both the current and antecedent year led to

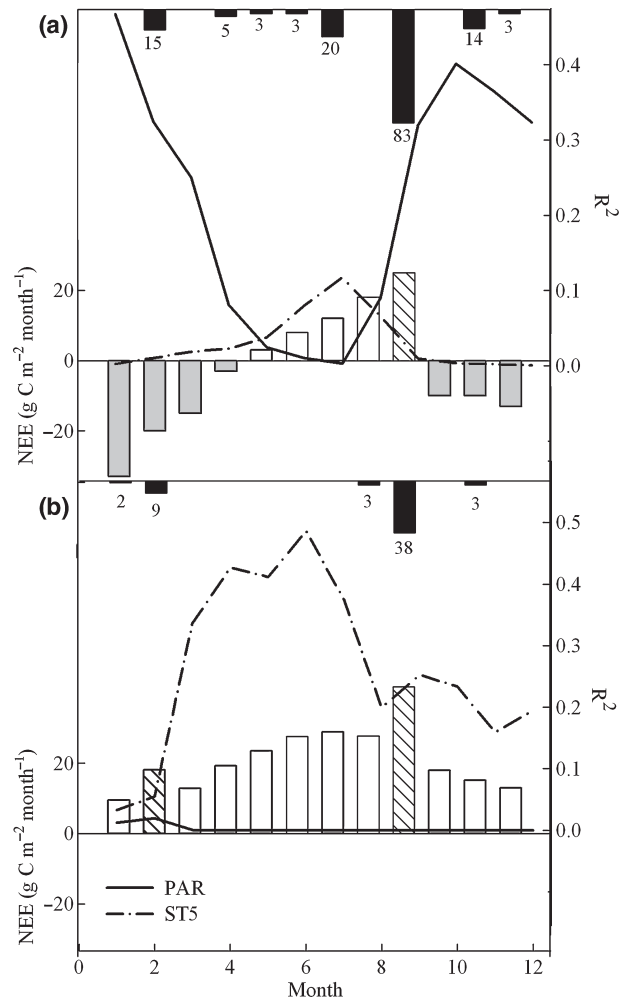


Fig. 4 (a) The year 2002 and (b) year 2005 monthly NEE shown as bars with associated R^2 values for photosynthetically active radiation by the solid line and ST5 by the dotted line. Gray bars represent growing season months, white bars represent dormant season months, and dashed bars represent storm months. Monthly precipitation (mm) is shown by the black bars at the top of each graph.

greater carbon uptake, with current year precipitation providing a greater influence ($NEE_x = -1.221 * \text{mm Precipitation}_{(x)} + -0.885 * \text{mm Precipitation}_{(x-1)} + 437.1$). A linear, but more comprehensive model considering both frequency and magnitude of precipitation events showed that significant relationships were sensitive to selection of the threshold for the definition of a precipitation event. Interannual variability of NEE was well captured with a minimum threshold of 1 mm per event on a daily basis and considering events from the current and antecedent year ($P = 0.04$) (Table 2). The relationship was also significant for a threshold of 2 mm, but became weaker for higher thresholds. A model with an event threshold of zero could not capture any

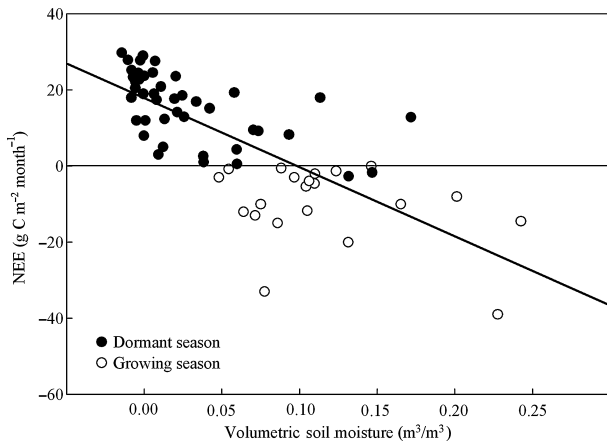


Fig. 5 Monthly NEE plotted against volumetric soil moisture at a depth of 5 cm. Open circles represent growing season months, whereas closed circles represent dormant season months from all study years.

variability, increasing only frequency but not adding to magnitude. If considering an additional year in the past or only current year rain events weaker correlations were found, in agreement with the initial model. It also showed that the frequency of events was a greater influence on annual NEE than precipitation magnitude, as inferred from the regression coefficients of 1.53 and -1.30 respectively. This implies a positive influence of event frequency on annual NEE as opposed to a negative influence of annual precipitation

magnitude on annual NEE (Fig. 7). The annual NEE sum of 171 g C m^{-2} for the year 2006 can be extrapolated from this interannual model, but care must be taken considering a high uncertainty ($\pm 103.9 \text{ g C m}^{-2}$ on the 95% confidence level) due to the simple model structure and the sparse sampling size.

Discussion

Seasonal diel carbon flux patterns

Past studies have reported the occurrence of two distinct seasons, which are referred to as the 'dry' dormant season and the 'wet' growing season that vary in length depending on the occurrence and magnitude of late summer monsoon events (Maya & Arriaga, 1996; Hastings *et al.*, 2005). A developed plant canopy characterizes growing season months, where photosynthetic activity is high and outpaces ecosystem respiration due to the availability of soil moisture and moderate temperatures, while dormant season months show a sparse canopy consisting of only evergreen shrubs and cacti. During the dormant season, the high soil temperatures stimulate ecosystem respiration, whereas low soil moisture contributes to limited photosynthesis (Raich & Tufekcioglu, 2000). The principle driver of carbon flux on a diel time scale can differentiate the seasonality of any particular month. Months in which half-hour average PAR was the most significant

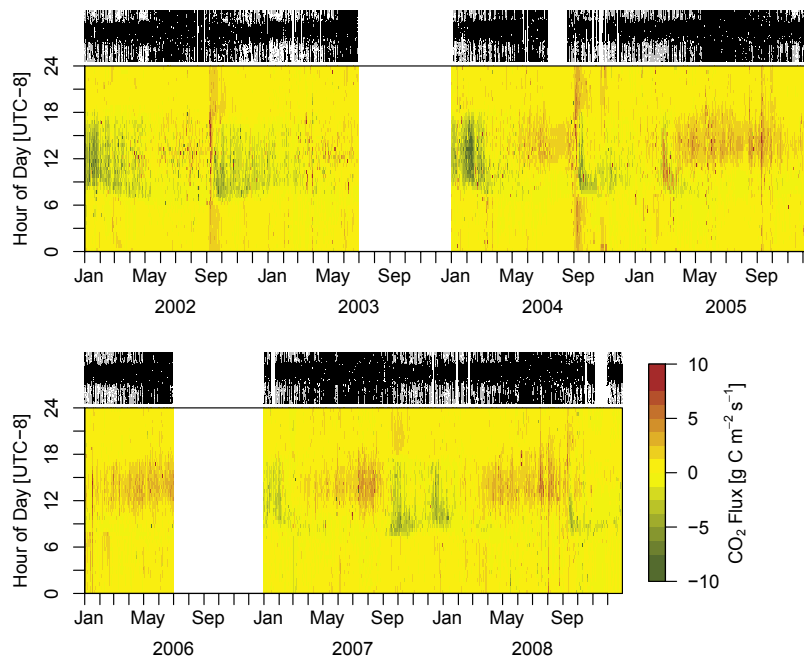


Fig. 6 Annual course of gap-filled NEE for years 2002–2008, in $\text{g C m}^{-2} \text{ d}^{-1}$. Data quality shown above plots with black signifying good data, gray for data removed due to u^* values below threshold of 0.15 m s^{-1} , and white for data missing due to instrument failure.

Table 2 Inter-annual NEE variability model output at different minimum precipitation thresholds and incorporating multiple years. R2 values for the current year (1 yr) and additional antecedent years. P values for the highest R2 value timespan, * represents a significant result. Modeled NEE for year 2006 at the highest R2 value timespan

Precipitation threshold (mm)	Precipitation events during study period	Modeled NEE year 2006 ($\text{g C m}^{-2} \text{yr}^{-1}$)	R^2		
			1 year	2 years	3 years
1	65	171	0.58	0.87*	0.74
2	49	243	0.75	0.90*	0.55
3	44	227	0.57	0.83	0.46
4	40	230	0.58	0.74	0.41

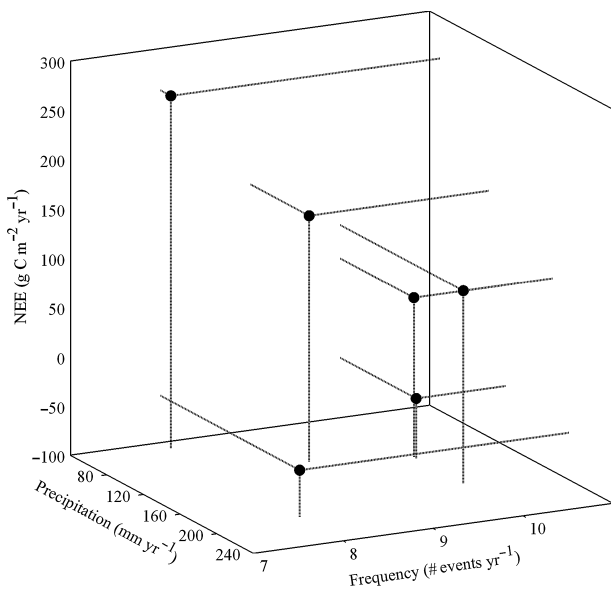


Fig. 7 3D scatter plot of annual NEE against annual precipitation magnitude and annual frequency of events.

meteorological factor controlling a sustained daylight CO_2 uptake were categorized as the growing season, whereas months in which half-hour average soil temperature at a depth of 5 cm (ST5) was the most significant meteorological factor to an increasing daylight CO_2 efflux were categorized as the dormant season. PAR was correlated well with diel carbon flux in the months following the monsoon rains of late summer and the small precipitation events that continued into early winter. Available water in the form of soil moisture supplied a dense canopy and allowed for PAR to be negatively correlated with carbon flux during this time period. Growing season months displayed a daytime carbon sink and a small nighttime source (Xu & Qi, 2001) (Fig. 3a). The nighttime source was temperature dependent as it followed the nocturnal decline in soil temperature (Rayment, 2000), and daytime uptake was interrupted by a photosynthetic decline due to

water stress in all months except those following a greater than average late summer monsoon event. This decline in autotrophic uptake ability is seen in other ecosystems due to water stress. For example, reduced stomatal conductance was observed in a water stressed Mediterranean ecosystem during afternoon hours in the dry season (Chaves *et al.*, 2002), and reduced maximal fluorescence was observed in a water stressed oak forest throughout the daylight hours, reaching a minimum between 1200 and 1300 h (Epron *et al.*, 1992).

Carbon flux in the dormant season months was always principally driven by ST5, where daytime carbon flux patterns show a small early morning uptake, when temperatures are lowest, followed by a large increase in source values as temperature rises throughout the day (Fig. 3b). The large daytime increase in carbon source strength was due to the positive relationship between soil microbial respiration and soil temperature and increased autotrophic respiration, as maintenance respiration increased to combat cellular damage due to the heat and light (Flanagan & Veum, 1974; Ryan, 1991). The large increase in carbon efflux values indicate that photosynthesis was maintained at very low levels or had ceased due to extreme water stress (Tezara *et al.*, 1999). This was confirmed by the flux-partitioning analysis that showed positive GPP values only during the first few hours after dawn during the dormant season followed by a rapid increase in ecosystem carbon source strength with only moderate increases in ecosystem respiration, which indicates a decrease in total photosynthesis. The point where this rapid increase in carbon source values was seen occurred earlier in the day as the dormant season progressed. This decrease in photosynthesis throughout the dormant season allows relatively small magnitudes of ecosystem respiration to dominate (Reichstein *et al.*, 2005). Bronson *et al.* (2011) demonstrated increased nighttime stomatal conductance and transpiration from Crassulacean acid metabolism (CAM) plants during June 2008 in Arizona, USA; however, no evidence of

sustained nighttime uptake was observed in this study. This may be due to low u^* values at night (excluded from analysis), which prevent the eddy covariance technique from accurately measuring small nocturnal sinks, or warm summer soil temperatures stimulating R_{eco} and masking CAM plant activity.

Drivers of seasonality and annual NEE

It is well known that arid ecosystems are water limited and that episodic precipitation events can cause a rapid shift of seasons (Noy-Meir, 1973; Lal, 2004; Hastings *et al.*, 2005); however, precipitation is primarily available to plant and microbial species as moisture in the soil. The magnitude and duration of soil moisture available at biologically important depths will largely dictate the magnitude and duration of the growing season. Seasonality is attributed to the occurrence of late summer storms providing precipitation needed for the formation of a vegetative canopy (Salinas-Zavala, 2002; Hastings *et al.*, 2005). This ecosystem presents a unique case in which the majority the annual precipitation falls in a usually single late summer monsoon event.

The importance of post-monsoon event frequency and the subsequent increases in soil moisture are dependent on the occurrence of a monsoon event large enough to stimulate plant growth. NDVI analysis of the study site showed a significant increase in green vegetation when measured against late summer precipitation magnitude. Years with a large monsoon event triggered greater canopy development and allowed for the utilization of soil moisture from later small precipitation events and the retention of that moisture through shading, as seen in the months following the September monsoon event in Fig. 4a (Potts *et al.*, 2010). Years with a small or nonexistent monsoon led to a reduced canopy, later small precipitation events were less important to photosynthesis and the system had drier soils throughout the typical growing season months. This led to the extension of the dormant season after the small September monsoon event in Fig. 4b. Thus, seasonal carbon balance seems to hinge on the late summer monsoon event, where a large monsoon provides the conditions necessary for long growing seasons and therefore more monthly carbon sinks, while years with small events had reduced canopies, drier soils, and displayed short or nonexistent growing seasons, leading to more monthly carbon sources.

As stated previously, the principle meteorological drivers of diel carbon flux, PAR, and ST5 can be used to classify each measured month as occurring during the growing or dormant season. Comparison of the monthly R^2 values of PAR and ST5 vs. monthly NEE displays a clear switching between the growing and

dormant seasons (Fig. 4). The year 2002 presents the seasonal pattern for this ecosystem explained by Hastings *et al.* (2005) characterized by annual carbon sinks. This pattern displays a period of plant growth during the fall and winter that is principally driven by PAR, following the late summer monsoon. This then transitions to a period of plant dormancy that is principally driven by ST5, following canopy loss in the spring and summer. The year 2002 had followed a year with especially heavy precipitation of 339 mm, which is evidenced by the long winter and spring growing season extending through April and beginning again after the late summer monsoons in September. Due to this long growing season and its associated photosynthesis, the year was an annual carbon sink (Wohlfahrt *et al.*, 2008). Presenting a contrast was the year 2005, which was especially dry and received only 55 mm of precipitation for the year and followed another dry year of 125 mm. The weak monsoon of year 2004 and lack of any large precipitation event in year 2005 led to a dramatically under-developed plant canopy. This reduced canopy was unable to take advantage of a winter storm in February or retain soil moisture, leading to a state of perpetual dormancy for the entire year and a large annual carbon source.

All years contained at least 1 month with a precipitation event following the dormant season, classified as storm months in the analysis. These precipitation events were usually the late summer monsoon, or a smaller winter storm during especially dry years. Flux-partitioning analysis showed that these events displayed high ecosystem respiration. This observation supports a strong microbial respiration response to large precipitation pulses after drought in arid systems (Huxman *et al.*, 2004).

Moisture in the upper soil layer (5 cm depth) is closely associated with monthly NEE, but it is the ecosystem response of canopy development to the late summer monsoon that allows for this moisture to be retained and utilized by the dominant plant species for photosynthesis. Large carbon sources during the dry summer can be assured every year (Fig. 2), so it is the length of the growing season that determines the magnitude of annual NEE sums. However, the variability in annual NEE during the study period cannot be fully explained by the magnitude of the monsoon event in the current year but is also subject to the condition of the ecosystem in the past.

Interannual variability of NEE

The annual NEE for this ecosystem was extremely variable over the study period with an average annual flux of $79 \pm 117 \text{ g C m}^{-2} \text{ yr}^{-1}$, as arid ecosystems are

highly sensitive to precipitation variability (Thomey *et al.*, 2011) (Table 1). In contrast, random uncertainties due to surface heterogeneity and a time-varying footprint, turbulence sampling errors, and errors associated with the measuring equipment were fairly low (not exceeding $5.0 \text{ g C m}^{-2} \text{ yr}^{-1}$ on the 95% confidence level), which can be explained by the lower flux magnitude compared with other sites.

Most meteorological variables were remarkably constant between years with the exception of precipitation and soil moisture. A series of years with small or missed monsoon events led to severe drought conditions, which were observed from late 2004 through the summer of year 2006. Drought conditions led to diminished photosynthesis during the growing season, as evidenced from comparing the average diel carbon flux patterns in January of 2004 to January of 2006 (Fig. 2). For example, January 2004 had followed a larger than average late summer precipitation events totaling 189 mm, and the large and sustained diel carbon uptake was the result of an ecosystem with relatively little water stress, while January 2006 had followed a smaller than average late summer precipitation event of 45 mm, which resulted in a monthly carbon source with no uptake observed from its average diel carbon pattern. As other meteorological variables were similar in 2004 and 2006, the area between the two uptake curves represents the potential carbon uptake lost due to water stress.

Higher annual precipitation, on average, correlated with a lower annual NEE, but could not fully explain carbon flux values for any one year, examining the annual NEE and precipitation for years 2004 and 2007 provides for a useful example. The year 2007 received 54 mm greater precipitation than the year 2004, but the ecosystem was a larger annual carbon source by 34 g C m^{-2} . However, when the past precipitation record is considered, the year 2004 followed years with higher overall precipitation while 2007 followed a period of severe drought that extended far into year 2006. Interestingly, frequency and magnitude of precipitation events over a 2 year timespan clearly capture most of the interannual variability of NEE (Table 2). Arguably, a more sophisticated nonlinear model could be found to model the underlying relationship, but the linear model presented here provides a simple, still significant representation. The frequency of events was associated with greater carbon loss and was relatively more important to annual NEE than the total magnitude of precipitation, which was associated with greater carbon uptake, for the current and antecedent year. As frequency of events increases, precipitation is spread over more, smaller events, possibly leading to a greater microbial respiration response seen in the storm

category months described above (Huxman *et al.*, 2004). These smaller events may not reach the threshold necessary to influence plant photosynthesis. As precipitation magnitude increases, there is a greater chance that the event will provide adequate soil moisture to allow for canopy development and a more pronounced growing season (Schwinning & Sala, 2004).

Ecosystem memory includes situations where the products of past productivity influence system responses to new precipitation inputs (Reynolds *et al.*, 2004; Schwinning *et al.*, 2004). This may be as simple as one year's productivity benefitting from the larger plant size and root area following a previous highly productive year. Or, it may be more complex, such as decades long lag effects through the decomposition of soil organic matter (Austin *et al.*, 2004). It is clear that not all interannual variability can be explained by a 2 year sliding window of precipitation magnitude and frequency, and it is undoubtedly necessary to investigate these patterns over even longer time periods to fully incorporate all significant cycles and controls on the carbon dynamics of this ecosystem. Still, a large percentage of the year-to-year variability in ecosystem carbon flux is explained based on soil moisture, PAR and soil temperature on a seasonal basis, and a 2 year sliding window of precipitation magnitudes and frequencies on an interannual basis.

The main meteorological variables that drive seasonal carbon flux in this ecosystem are functions of this strong relationship with soil moisture. Increased soil moisture stimulates canopy development and can enhance the length of the growing season and allow for the utilization of the abundant year-round PAR. A longer growing season also provides for lower soil temperatures through shading and evaporative cooling and establishes conditions to more efficiently utilize future precipitation. Any discussion of arid system carbon dynamics must take prior conditions and high interannual variability of NEE into account before assessments of long-term arid land source/sink strength are made.

Acknowledgements

This study was funded in part by the National Science Foundation (INT-072140, DUE-9952816, and DGE-0139378) and by a binational grant from Consejo Nacional de Ciencia y Tecnología, Mexico (J200.179/2002). David Lipson was invaluable for soil respiration and moisture advice. Technical and or processing support is appreciated from Luis Carlos Moreno-Galvan, Larry Miller, and Juan Vega-Mayagoitia at the Centro de Investigaciones Biológicas del Noroeste (CIBNOR), Rommel Zulueta, and Hiroki Ikawa at San Diego State University. Flux-partitioning advice is appreciated from Cove Sturtevant. We also acknowledge the Biogeochemical Model-Data Integration Group at the Max Planck Institute for Biogeochemistry in Jena for providing

the online gap-filling and flux-partitioning tool. Long-term access to the ecological reserve at the Centro de Investigaciones Biológicas del Noroeste and in-kind support by CIBNOR was critical to the success of this project. Initial support including provision of fiber optic cable to the site, servers at CIBNOR, and a secure concrete field building were critical to the success of this project. None of this would have been possible without the early belief and support of previous CIBNOR Director Dr. Mario Martinez and Ms. Elena Enriquez and continuing support by current Director Dr. Sergio Hernandez.

References

- Allard V, Ourcival JM, Rambal S, Joffre R, Rocheteau A (2008) Seasonal and annual variation of carbon exchange in an evergreen Mediterranean forest in southern France. *Global Change Biology*, **14**, 714–725.
- Archibald SA, Kirton A, Merwe MR, van der Scholes RJ, Williams CA, Hanan N (2009) Drivers of inter-annual variability in Net Ecosystem Exchange in a semi-arid savanna ecosystem, South Africa. *Biogeosciences*, **6**, 251–266.
- Arneth A, Veenendaal EM, Best C, Timmermans W, Kolle O, Montagnani L, Shibistova O (2006) Water use strategies and ecosystem-atmosphere exchange of CO₂ in two highly seasonal environments. *Biogeosciences*, **3**, 421–437.
- Asner GP, Archer S, Hughes RF, Ansley RJ, Wessman CA (2003) Net changes in regional woody vegetation cover and carbon storage in Texas Drylands, 1937–1999. *Global Change Biology*, **9**, 316–335.
- Austin AT, Yahdjian L, Stark JM *et al.* (2004) Water pulses and biogeochemical cycles in arid and semiarid ecosystems. *Oecologia*, **141**, 221–235.
- Baldocchi DD (2003) Assessing the eddy covariance technique for evaluating carbon dioxide exchange rates of ecosystems: past, present and future. *Global Change Biology*, **9**, 479–492.
- Baldocchi DD, Wilson KB (2001) Modeling CO₂ and water vapor exchange of a temperate broadleaved forest across hourly to decadal time scales. *Ecological Modelling*, **142**, 155–184.
- Baldocchi DD, Hicks BB, Meyers TP (1988) Measuring biosphere-atmosphere exchanges of biologically related gases with micrometeorological methods. *Ecology*, **69**, 1331–1340.
- Baldocchi DD, Falge E, Gu L *et al.* (2001) FLUXNET: A New tool to study the temporal and spatial variability of ecosystem-scale carbon dioxide, water vapor, and energy flux densities. *Bulletin of the American Meteorological Society*, **82**, 2415–2434.
- Barford CC, Wofsy SC, Goulden ML *et al.* (2001) Factors controlling long- and short-term sequestration of atmospheric CO₂ in a mid-latitude forest. *Science*, **294**, 1688–1691.
- Braswell BH, Schimel DS, Linder E *et al.* (1997) The response of global terrestrial ecosystems to interannual temperature variability. *Science*, **278**, 870–872.
- Bronson DR, English NB, Dettman DL, Williams DG (2011) Seasonal photosynthetic gas exchange and water-use efficiency in a constitutive CAM plant, the giant saguaro cactus (*Carnegiea gigantea*). *Oecologia*, **167**, 861–871.
- Brown DE, Lowe CH (1980) Map, biotic communities of the southwest. Rocky Mt. Forest and Range Expt. Station General Tech Report RM-78, USDA Forest Service, Fort Collins, CO, USA.
- Chaves MM, Pereira JS, Maroco J *et al.* (2002) How plants cope with water stress in the field. Photosynthesis and growth. *Annals of Botany*, **89**, 907–916.
- CONAGUA (2011) Estadísticas del agua en México. Ed. 2011. Comisión Nacional del Agua. Insurgentes Sur No. 2416, Col. Copilco el Bajo C.P. 04340, Coyoacán, México, D.F. Available at: <http://www.conagua.gob.mx> (accessed 20 October 2011).
- Connin SL, Virginia RA, Chamberlain CP (1997) Carbon isotopes reveal soil organic matter dynamics following arid land shrub expansion. *Oecologia*, **110**, 374–386.
- Emmerich W (2003) Carbon dioxide fluxes in a semiarid environment with high carbonate soils. *Agricultural and Forest Meteorology*, **116**, 91–102.
- Epron D, Dreyer E, Breda N (1992) Photosynthesis of oak trees [*Quercus petraea* (Matt) Liebl] during drought under field conditions: diel course of net CO₂ assimilation and photochemical efficiency of photosystem II. *Plant, Cell and Environment*, **15**, 809–820.
- Eswaran H, Reich PF, Kimble JM *et al.* (2000) Global carbon sinks. In: *Global Climate Change and Pedogenic Carbonates*, (eds Lal R, Kimble JM, Eswaran H, Stewart BA), pp. 15–26. CRC Press, Boca Raton, FL.
- Falge E, Baldocchi DD, Olson R *et al.* (2001) Gap filling strategies for long term energy flux data sets. *Agricultural and Forest Meteorology*, **107**, 71–77.
- Flanagan PW, Veum AK (1974) Relationships between respiration, weight loss, temperature and moisture in organic residues on tundra. In: *Soil Organisms and Decomposition in Tundra*, (eds Heal OW, Maclean Jr. SF, Holding AJ), pp. 249–277. IBP Tundra Biome Steering Committee, Stockholm, Sweden.
- García E (1973) *Modificaciones al Sistema de clasificación climática de Koepen (para adaptarlo a las condiciones de la República Mexicana)* (2nd edn). Instituto de Geografía, UNAM, Mexico.
- Goulden ML, Munger JW, Fan SM, Daube BC, Wofsy SC (1996) Exchange of carbon dioxide by a deciduous forest: response to interannual climate variability. *Science*, **271**, 1576–1578.
- Grunzweig JM, Lin T, Rotenberg E, Schwartz A, Yakir D (2003) Carbon sequestration in arid-land forest. *Global Change Biology*, **9**, 791–799.
- Gutiérrez-Ruacho OG, Brito-Castillo L, Díaz-Castro SC, Watts CJ (2010) Trends in rainfall and extreme temperatures in northwestern Mexico. *Climate Research*, **42**, 133–142.
- Hastings SJ, Oechel WC, Muhlia-Melo A (2005) Diel, seasonal and annual variation in the net ecosystem CO₂ exchange of a desert shrub community (Sarcocaulis) in Baja California, Mexico. *Global Change Biology*, **11**, 927–939.
- Huenneke LF, Anderson JP, Remmenga M, Schlesinger WH (2002) Desertification alters patterns of aboveground net primary production in Chihuahuan ecosystems. *Global Change Biology*, **8**, 247–264.
- Huxman TE, Snyder KA, Tissue D *et al.* (2004) Precipitation pulses and carbon fluxes in semiarid and arid ecosystems. *Oecologia*, **141**, 254–268.
- Lal R (2004) Carbon sequestration in dryland ecosystems. *Environmental management*, **33**, 528–544.
- León de la Luz JL, Navarro-Perez JJ, Solís-Cámarra AB (2000) Vegetation of the lowlands of the Cape Region, Baja California Sur: a transitional xerophytic tropical plant community. *Journal of Vegetation Science*, **11**, 35–39.
- Luo H, Oechel WC, Hastings SJ, Zulueta R, Qian Y, Kwon H (2007) Mature semiarid chaparral ecosystems can be a significant sink for atmospheric carbon dioxide. *Global Change Biology*, **13**, 386–396.
- Ma S, Baldocchi D, Xu L, Hehn T (2007) Inter-annual variability in carbon dioxide exchange of an oak/grass savanna and open grassland in California. *Agricultural and Forest Meteorology*, **147**, 157–171.
- McMillen RT (1988) An eddy-correlation technique with extended applicability to non-simple terrain. *Boundary-Layer Meteorology*, **43**, 231–245.
- Maya Y, Arriaga L (1996) Litterfall and phenological patterns of the dominant overstorey species of a desert scrub community in north-western Mexico. *Journal of Arid Environments*, **34**, 23–35.
- Morgenstern K, Black TA, Humphreys ER *et al.* (2004) Sensitivity and uncertainty of the carbon balance of a Pacific Northwest Douglas-fir forest during an El Niño/La Niña cycle. *Agricultural and Forest Meteorology*, **123**, 201–219.
- Noy-Meir I (1973) Desert ecosystems: environment and producers. *Annual Review of Ecology and Systematics*, **4**, 25–51.
- Odum EP (1969) The strategy of ecosystem development. *Science*, **164**, 262–270.
- Perea MC, Ezcurra E, León de la Luz JL (2005) Functional morphology of a sarcocaulis desert scrub in the bay of La Paz, Baja California Sur, Mexico. *Journal of Arid Environments*, **62**, 413–426.
- Potts DL, Huxman TE, Cable JM *et al.* (2006) Antecedent moisture and seasonal precipitation influence the response of canopy-scale carbon and water exchange to rainfall pulses in a semi-arid grassland. *New Phytologist*, **170**, 849–860.
- Potts DL, Scott RL, Bayram S, Carbonara J (2010) Woody plants modulate the temporal dynamics of soil moisture in a semi-arid mesquite savanna. *Ecology*, **3**, 20–27.
- Raich JW, Tufekcioglu A (2000) Vegetation and soil respiration: correlations and controls. *Biogeochemistry*, **48**, 71–90.
- Rayment MB (2000) Investigating the role of soils in terrestrial carbon balance: harmonizing methods for measuring soil CO₂ efflux. LESC exploratory workshop, Edinburgh, 6–8 April, 2000, European Science Foundation, Edinburgh, UK.
- Reichstein M, Falge E, Baldocchi D *et al.* (2005) On the separation of net ecosystem exchange into assimilation and ecosystem respiration: review and improved algorithm. *Global Change Biology*, **11**, 1–16.
- Reynolds JF, Kemp PR, Ogle K, Fernández RJ (2004) Modifying the 'pulse-reserve' paradigm for deserts of North America: precipitation pulses, soil water, and plant responses. *Oecologia*, **141**, 194–210.
- Richardson AD, Mahecha MD, Falge E *et al.* (2008) Statistical properties of random CO₂ flux measurement uncertainty inferred from model residuals. *Agricultural and Forest Meteorology*, **148**, 38–50.
- Rotenberg E, Yakir D (2010) Contribution of semi-arid forests to the climate system. *Science*, **327**, 451–454.

- Ryan MG (1991) Effects of climate change on plant respiration. *Ecological Applications*, **1**, 157–167.
- Salinas-Zavala C (2002) Interannual variability of NDVI in northwest Mexico Associated climatic mechanisms and ecological implications. *Remote Sensing of Environment*, **82**, 417–430.
- Schlesinger WH, Reynolds JF, Cunningham GL, Huenneke LF, Jarrell WM, Virginia RA, Whitford WG (1990) Biological feedbacks in global desertification. *Science*, **247**, 1043–1048.
- Schlesinger WH, Belnap J, Marion G (2009) On carbon sequestration in desert ecosystems. *Global Change Biology*, **15**, 1488–1490.
- Schwinning S, Sala OE (2004) Hierarchy of responses to resource pulses in arid and semi-arid ecosystems. *Oecologia*, **141**, 211–220.
- Schwinning S, Sala OE, Loik ME, Ehleringer JR (2004) Thresholds, memory, and seasonality: understanding pulse dynamics in arid/semi-arid ecosystems. *Oecologia*, **141**, 191–193.
- Seely MK, Louw GN (1980) First approximation of the effects of rainfall on the ecology and energetics of a Namib Desert dune ecosystem. *Journal of Arid Environments*, **3**, 25–54.
- Shreve F, Wiggins IL (1964) *Vegetation and Flora of the Sonoran Desert*, Vol 2. Stanford University Press, Stanford, CA.
- Tezara W, Mitchell VJ, Driscoll SD, Lawlor DW (1999) Water stress inhibits plant photosynthesis by decreasing coupling factor and ATP. *Nature*, **401**, 914–917.
- Thomey M, Collins SL, Vargas R, Johnson J, Brown R, Natvig D, Friggs M (2011) Effect of precipitation variability on net primary production and soil respiration in a Chihuahuan desert grassland. *Global Change Biology*, **17**, 1505–1515.
- Troyo-Diéquez E, De Lachica-Bonilla F, Fernández-Zayas JL (1990) A simple aridity equation for agricultural purposes in marginal zones. *Journal of Arid Environments*, **19**, 353–362.
- Unland H (1996) Surface flux measurement and modeling at a semi-arid Sonoran Desert site. *Agricultural and Forest Meteorology*, **82**, 119–153.
- Vargas R, Yopez E (2011) Toward a Mexican eddy covariance network for Carbon Cycle Science. *Eos, Transactions American Geophysical Union*, **92**, 307.
- Webb EK, Pearman GI, Leuning R (1980) Corrections of flux measurements for density effects due to heat and water vapor transfer. *Quarterly Journal of the Royal Meteorological Society*, **106**, 85–100.
- Wilson KB, Goldstein A, Falge E *et al.* (2002) Energy balance closure at FLUXNET sites. *Agricultural and Forest Meteorology*, **113**, 223–243.
- Wohlfahrt G, Fenstermaker LF, Arnone JA (2008) Large annual net ecosystem CO₂ uptake of a Mojave Desert ecosystem. *Global Change Biology*, **14**, 1475–1487.
- Xu M, Qi Y (2001) Soil-surface CO₂ efflux and its spatial and temporal variations in a young ponderosa pine plantation in northern California. *Global Change Biology*, **7**, 667–677.